Research on the Laminar Inlet of a Pipe with Annular Space

メタデータ	言語: eng 出版者: 公開日: 2013-10-29 キーワード (Ja): キーワード (En): 作成者: Sugino, Eitaro メールアドレス: 所属:
URL	https://doi.org/10.24729/00008239

Research on the Laminar Inlet of a Pipe with Annular Space

by

Eitaro SUGINO*

(Received September 30, 1967)

The Navier-Stokes equation is linearized for the steady flow in the laminar inlet of a pipe with annular space. This solution shows the family of velocity profiles defined by the modified Bessel functions. By applications of this family to the momentum equation and the energy equation respectively, the inlet length and the pressure drop are presented. Some examples of computation are given for the ratio of the inner and outer radii of annular space, $m=1.2\sim5$. The results of computation prove that the relation between the dimensionless distance from pipe entrance $\sigma=x/(R_2-R_1)Re$ and the pressure drop $(p_0-p)/(\rho u_0^2/2)$ is almost unaffected by m, and that the inlet length σ_L is also unaffected. Practically, σ_L may be evaluated to be 0.02.

Some experimental results for the pressure drop, which have been made by the use of water and air, are compared with the present analysis. The measured values have a good agreement with the analytical values near the entrance, but are lower than the analytical values for downstream by about 10%. Experimentally the inlet length σ_L may be observed to be $0.05\sim0.06$.

1. Introduction

At the industrial plants, many heat exchangers for heating or cooling are used. The method of the heat transfer by circular pipe, parallel plates or annular pipes is a particularly important and basic problem. The most generalized method for analysis of this problem is that which calculates the temperature distribution, the heat transfer coefficient, etc. of the thermal inlet by using the velocity profiles of the velocity inlet of fluid.

For circular pipe, some solutions are presented by Kays(1) and Sibahayasi-Sugino(2). Solutions for parallel plates are given by Cess-Shaffer(3), Han(4), and Siegel-Sparrow(5). Murakawa(6) obtained a solution for annular pipes. This method is based on his solution(7) for the velocity inlet, but his results do not appear to be useful. Roy(8) has presented a solution for the laminar velocity inlet of annular pipes. However, Langhaar's method(9) for the velocity inlet of circular pipe seems to be more effective in obtaining the solution of the velocity inlet which is fundamental for the heat transfer problem. Han(10) has applied Langhaar's method to obtain the velocity profile for the parallel plates. Kays(1) utilized also Langhaar's solution in the heat transfer problem for the circular pipe. Then, Langhaar's method is applied on the present investigation for the annular pipes. This method linearizes the Navier-Stokes equation and presents the velocity profiles which are defined by the modified Bessel functions. Applications of this profiles to the momentum equation and the energy equation give the inlet length and the pressure drop. Some examples of numerical calculations are shown for the three values of radius ratio, $m=1.2$, 2 and 5.

Moreover, the experiment by water and air when $m=1.0967$ and 1.2699 is made in order to compare with the analytical results of pressure drop.

2. Nomenclature

The nomenclatures in this investigation are as follows.

g_x : component of gravitational acceleration in axial direction
I_n : modified Bessel function of the first kind of the n th order

* Department of Mechanical Engineering.

K_n : modified Bessel function of the second kind of the n th order
$m=R_2/R_1$: ratio of inner and outer radii of annular space
$\bar{m}=\bar{R}/R_1$
p : static pressure of fluid in arbitrary cross section
p_0 : static pressure of fluid at pipe entrance
r : radius from pipe center
R_1 : inner radius of annular space
R_2 : outer radius of annular space
$\bar{R}=(R_1+R_2)/2$: average radius of annular space
$Re=(R_2-R_1)u_0/\nu$: Reynolds number
$t=r\beta$: parameter of modified Bessel function
$t_1=R_1\beta$
u : velocity component in axial direction
u_0 : mean velocity
$\bar{u}$: value of u at $r=\bar{R}$
v : velocity component in radial direction
x : distance from pipe entrance in axial direction
α, β: functions of x only
$\lambda=u/u_0$
$\bar{\lambda}=\bar{u}/u_0$
μ : coefficient of viscosity of fluid
ν : kinematic coefficient of viscosity of fluid
ρ : mass density of fluid
$\sigma=x/(R_2-R_1)Re$: dimensionless distance from pipe entrance
σ_L : dimensioneless inlet length

3. Velocity Distribution

The Navier-Stokes equation for the steady flow, which flows in axial direction through an annular space without rotating motion, is

$$u\frac{\partial u}{\partial x}+v\frac{\partial u}{\partial r}=g_x-\frac{1}{\rho}\frac{\partial p}{\partial x}+\nu\left(\frac{\partial^2 u}{\partial r^2}+\frac{1}{r}\cdot\frac{\partial u}{\partial r}+\frac{\partial^2 u}{\partial x^2}\right) \quad (1)$$

Neglecting $\partial^2 u/\partial x^2$ and assuming p as a function of x only,

$$u\frac{\partial u}{\partial x}+v\frac{\partial u}{\partial r}=g_x-\frac{1}{\rho}\frac{dp}{dx}+\nu\left(\frac{\partial^2 u}{\partial r^2}+\frac{1}{r}\frac{\partial u}{\partial r}\right) \quad (2)$$

Boundary conditions are as follows.

i) $u=0$ for $r=R_1$ (3)

ii) $u=0$ for $r=R_2$ (4)

iii) $u=v_0$ for $x=0$ (5)

From the equation of continuity,

$$\int_{R_1}^{R_2} 2\pi r u dr=\pi(R_2{}^2-R_1{}^2)u_0 \quad (6)$$

According to the Langhaar's method, the following substitution is made by α and β, which are functions of x only.

$$u\frac{\partial u}{\partial x}+v\frac{\partial u}{\partial r}=\nu\beta^2 u \quad (7)$$

$$g_x-\frac{1}{\rho}\frac{dp}{dx}=-\nu\alpha \quad (8)$$

This substitution may be permitted for the following reasons:

i) At all points on the pipe wall surface, since $u=v=0$, Eq. (7) is satisfied for every value of β.

ii) In the fully developed flow region beyond the inlet length, $\beta=0$ results and Eq. (7) is satisfied.

iii) Since it may be considered that v and $\partial u/\partial r$ do not exist and u is a function of x only in the core flow, Eq. (7) becomes effective in the form $\partial u/\partial x=\nu\beta^2$.

iv) Since it may be considered that the boundary layer does not exist at the pipe entrance $x=0$ and that $\partial u/\partial r=0$, Eq. (7) is also satisfied in the form $\partial u/\partial x=\nu\beta^2$ at all points of the cross section of the pipe entrance.

Namely, Eq. (7) is justified except for the points in the boundary layer near the pipe wall. Then, substituting Eqs. (7) and (8) for Eq. (2)

$$\frac{\partial^2 u}{\partial r^2}+\frac{1}{r}\frac{\partial u}{\partial r}-\beta^2 u = \alpha \tag{9}$$

Putting $t=r\beta$,

$$\frac{\partial^2 u}{\partial t^2}+\frac{1}{t}\frac{\partial u}{\partial t}-u = \frac{\alpha}{\beta^2} \tag{10}$$

The solution of Eaq. (10) is

$$u = A\,I_0(t)+B\,K_0(t)-\alpha/\beta^2 \tag{11}$$

The integral constants A, B and α/β^2 can be determined by the boundary conditions (3), (4) and the equation of continuity, and the dimensionless velocity profile is as follows:

$$\lambda = \frac{u}{u_0} = \frac{(m^2-1)\{q_0 I_0(t)+q_1 K_0(t)+q_2\}}{h(t_1)} \tag{12}$$

where

$$q_0 = K_0(t_1)-K_0(mt_1) \tag{13}$$

$$q_1 = I_0(mt_1)-I_0(t_1) \tag{14}$$

$$q_2 = I_0(t_1)K_0(mt_1)-I_0(mt_1)K_0(t_1) \tag{15}$$

$$h(t_1) = q_0\{I_2(t_1)-m^2 I_2(mt_1)\}+q_1\{K_2(t_1)-m^2 K_2(mt_1)\} \tag{16}$$

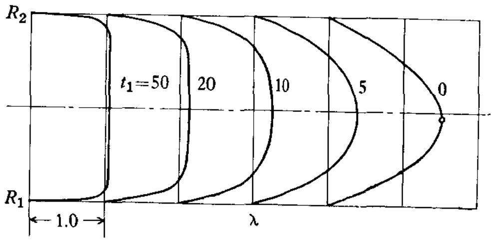

Fig. 1. Velocity profiles ($m=2$)

Fig. 1 shows the velocity profiles for $m=2$, and proves that the velocity profile approaches to that of the fully developed flow, in accordance with smaller value of t_1 or with the increasing of distance from entrance. The maximum velocity point deviates inward and this deviation becomes larger as the value of m grows larger.

When $t_1=0$ ($\beta=0$), it means the end of inlet. In this case, Eq. (12) results in

$$\lim_{t_1\to 0}\lambda = \frac{2\,[(m^2-1)\log(t/t_1)-\{(t/t_1)^2-1\}\log m]}{(m^2+1)\log m-(m^2-1)} \tag{17}$$

This result coincides perfectly with the theoretical velocity distribution[11] in the fully developed flow.

4. Distance from Entrance

By the integrating of Eq. (2) over an arbitrary cross section, the momentum equation results in

$$2\frac{d}{dx}\int_{R_1}^{R_2} u^2 r dr = \left(g_x - \frac{1}{\rho}\frac{dp}{dx}\right)(R_2^2 - R_1^2) + 2\nu\int_{R_1}^{R_2}\left(r\frac{\partial^2 u}{\partial r^2} + \frac{\partial u}{\partial r}\right)dr \tag{18}$$

Since the core flow is almost unaffected by viscosity, the following equation may be approximately justified at the center of annular space $r=\bar{R}$[12] from Eq. (2).

$$g_x - \frac{1}{\rho}\frac{dp}{dx} = \bar{u}\frac{\partial \bar{u}}{\partial x} \tag{19}$$

Substituting this equation for Eq. (18),

$$2\nu\int_{R_1}^{R_2}\left(r\frac{\partial^2 u}{\partial r^2} + \frac{\partial u}{\partial r}\right)dr + \frac{d}{dx}\int_{R_1}^{R_2}(\bar{u}^2 - 2u^2) r dr = 0 \tag{20}$$

From Eq. (12),

$$\frac{d}{dx}\int_{R_1}^{R_2}(\bar{u}^2 - 2u^2) r dr = \frac{d}{d\sigma}\left[\frac{\nu u_0}{(m-1)^2 t_1^2}\int_{t_1}^{m t_1}(\bar{\lambda}^2 - 2\lambda^2)\, t dt\right]$$

$$= -\nu u_0 \frac{d}{d\sigma}\left[\left\{\frac{m+1}{h(t_1)}\right\}^2\left\{2q_2 h(t_1) - \frac{m^2-1}{2}q_3^2 - m^2 q_4^2 + q_5^2\right\}\right] \tag{21}$$

$$2\nu\int_{R_1}^{R_2}\left(r\frac{\partial^2 u}{\partial r^2} + \frac{\partial u}{\partial r}\right)dr = \frac{2\nu u_0 t_1 (m^2-1)(m q_4 - q_5)}{h(t_1)} \tag{22}$$

where

$$q_3 = q_0 I_0(\bar{m} t_1) + q_1 K_0(\bar{m} t_1) + q_2 \tag{23}$$

$$q_4 = q_0 I_1(m t_1) - q_1 K_1(m t_1) \tag{24}$$

$$q_5 = q_0 I_1(t_1) - q_1 K_1(t_1) \tag{25}$$

Sbustituting Eqs. (21) and (22) for Eq. (20) and arranging,

$$-1/g(t_1) = df(t_1)/d\sigma \tag{26}$$

where

$$f(t_1) = \left\{\frac{m+1}{h(t_1)}\right\}^2\left\{2q_2 h(t_1) - \frac{m^2-1}{2}q_3^2 - m^2 q_4^2 + q_5^2\right\} \tag{27}$$

$$g(t_1) = \frac{h(t_1)}{2(m^2-1)t_1(q_5 - m q_4)} \tag{28}$$

From Eq. (12),

$$\lim_{t_1\to\infty}\lambda = 1 \tag{29}$$

When the boundary condition (5) is substantiated, it should be as follows:

$$\lim_{t_1\to\infty}\sigma(t_1) = 0 \tag{30}$$

Consequently, from Eq. (26),

$$\sigma = -\int_{t_1=\infty}^{t_1=t_1} g(t_1)\,df(t_1) = \int_{t_1=t_1}^{t_1=\infty} g(t_1)\,df(t_1) \tag{31}$$

Moreover, from Eqs. (27) and (28),

$$\lim_{t_1\to\infty} f(t_1) = \frac{1}{2}+\frac{1}{m-1} \tag{32}$$

$$\lim_{t_1\to\infty} g(t_1) = 0 \tag{33}$$

$$\lim_{t_1\to 0} f(t_1) = \frac{m+1}{(m-1)\{(m^2+1)\log m-(m^2-1)\}^2}\Big[\frac{4}{3}(m^4+m^2+1)(\log m)^2$$
$$-\frac{1}{8}(m-1)^2(m+3)^2(\log m)^2-3(m^4-1)\log m+2(m^2-1)^2\{1-(\log \bar{m})^2\}$$
$$+(m+1)(m-1)^2(m+3)\log m\cdot\log \bar{m}\Big] \tag{34}$$

$$\lim_{t_1\to 0} g(t_1) = \frac{(m^2+1)\log m-(m^2-1)}{8(m^2-1)\log m} \tag{35}$$

Accordingly, Eq. (31) becomes

$$\sigma = \int_{f(t_1)}^{1/2+1/(m-1)} g(t_1)df(t_1) \tag{36}$$

If the value of m is given, $g(t_1)$ and $f(t_1)$ can be evaluated for various values of t_1 from Eqs. (27) and (28). By the selection of t_1 with proper intervals and by the numerical integration of Eq. (36), the values of σ which correspond with each value of t_1 are obtained. And the inlet length is as follows.

$$\sigma_L = \lim_{t_1\to 0}\sigma(t_1) = \int_{\lim_{t_1\to 0} f(t_1)}^{1/2+1/(m-1)} g(t_1)df(t_1) \tag{37}$$

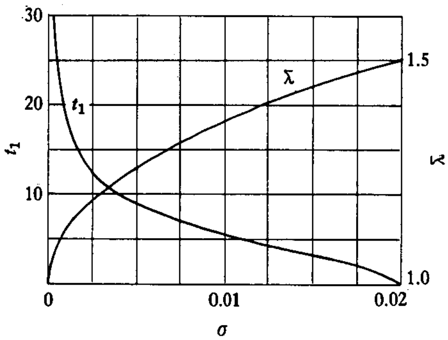

Fig. 2. t_1 and $\bar{\lambda}$ $(m=2)$

For example, the calculated results of σ and $\bar{\lambda}$ for $m=1.2$, $m=2$ and $m=5$ are indicated in Fig. 2 and Tables 1 to 3. And the inlet length is almost unaffected by the value of m, as shown in Table 4. Practically, σ_L may be evaluated to be 0.02.

5. Pressure Drop

The pressure drop in a horizontal annular space is due to the fluid friction and the change of the kinetic energy. Therefore, the energy equation per unit time is

$$(R_2^2-R_1^2)u_0(p_0-p) = 2\mu\int_0^x dx\int_{R_1}^{R_2}\Big(\frac{\partial u}{\partial r}\Big)^2 rdr+\rho\int_{R_1}^{R_2}(u^3-u_0^3)rdr \tag{38}$$

Integrating the first term of the right side in the above by the substitution of Eq. (12), and transforming this into the dimensionless,

$$\frac{p_0-p}{\rho u_0^2/2} = \int_0^\sigma \Phi(t_1)d\sigma+\frac{2}{(m^2-1)t_1^2}\int_{t_1}^{mt_1}(\lambda^3-1)tdt \tag{39}$$

where

$$\Phi(t_1) = 2(m+1)(m-1)^3\left\{\frac{t_1}{h(t_1)}\right\}^2\left\{m^2q_4^2-q_5^2-q_2h(t_1)\right\} \tag{40}$$

Since $\Phi(t_1)\to\infty$ for $\sigma\to 0\ (t_1\to\infty)$, the first term of the right side of Eq. (39) can not be integrated. However, the following approximate expression is effective for a sufficiently larger value of t_1.

$$\int_0^\sigma \Phi(t_1)d\sigma = \frac{2(m+1)(m-1)^2}{t_1} - \frac{(m^2-1)(9m^4+12m^3-490m^2+12m+9)}{32m^2t_1^2} \tag{41}$$

Now, $t_1=2500$ is selected for $m=1.2$, $t_1=50000$ for $m=2$, and $t_1=2500000$ for $m=5$. Then, next results are given.

i) $m=1.2$:

$$\int_0^\sigma \Phi(t_1)d\sigma = 0.000\ 071\ 4+\int_{0.99\times 10^{-6}}^\sigma \Phi(t_1)d\sigma \tag{42}$$

ii) $m=2$:

$$\int_0^\sigma \Phi(t_1)d\sigma = 0.000\ 120\ 0+\int_{0.10\times 10^{-9}}^\sigma \Phi(t_1)d\sigma \tag{43}$$

iii) $m=5$:

$$\int_0^\sigma \Phi(t_1)d\sigma = 0.000\ 076\ 8+\int_{0.25\times 10^{-14}}^\sigma \Phi(t_1)d\sigma \tag{44}$$

Each second term of the right side in Eqs. (42) to (44) can be estimated by the numerical method. The second term of the right side in Eq. (39) can be computed by Simpson's rule with the substitution of Eq. (12). Thus, the pressure drop for $\sigma<\sigma_L$ is obtained. Some examples of the calculated results are shown in Table 1 to 3 and Fig. 3. It may be considered that the pressure

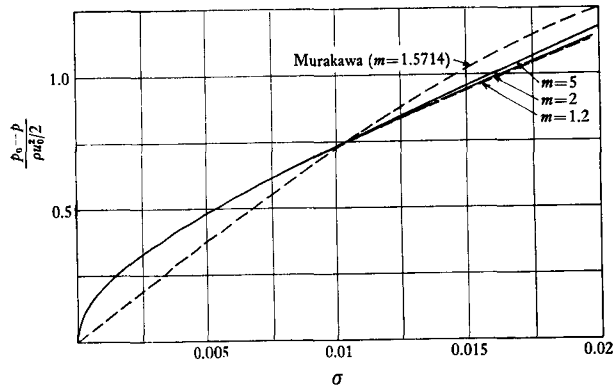

Fig. 3. Calculated results of pressure drop

drop is almost unaffected by m, as shown in Fig. 3. The calculated results by Murakawa(7) are appended to this figure for comparison, and his results appear to be too small near the pipe entrance.

When σ is larger than the inlet length σ_L, from Eq. (40),

$$\int_{\sigma_L}^\sigma \lim_{t_1\to 0}\Phi(t_1)d\sigma = \frac{16(m-1)^2\log m}{(m^2+1)\log m-(m^2-1)}(\sigma-\sigma_L) \tag{45}$$

This coincides perfectly with the theoretical value of the fully developed flow(11). This result leads to the following form of the pressure drop for $\sigma>\sigma_L$.

$$\frac{p_0-p}{\rho u_0^2/2} = C_1\sigma+C_2 \tag{46}$$

Table 1. $m=1.2$

t_1	σ	$\bar{\lambda}$	$\frac{p_0-p}{\rho u_0^2/2}$
∞	0	1.000 0	0
2 500	0.000 000 99	1.004 0	0.004 769
750	0.000 011 51	1.013 5	0.021 09
250	0.000 113 8	1.041 7	0.068 73
200	0.000 183 9	1.052 6	0.085 68
100	0.000 863 9	1.111 0	0.189 4
70	0.001 955	1.164 5	0.287 2
50	0.004 006	1.233 1	0.422 2
40	0.005 997	1.284 2	0.532 0
30	0.009 068	1.347 7	0.680 8
25	0.011 06	1.382 6	0.772 6
20	0.013 28	1.417 5	0.867 2
15	0.015 56	1.449 8	0.963 3
10	0.017 62	1.476 4	1.049 6
5	0.019 08	1.494 0	1.106 6
2	0.019 53	1.499 2	1.124 4
0	0.019 62	1.500 2	1.132 1

Table 2. $m=2$

t_1	σ	$\bar{\lambda}$	$\frac{p_0-p}{\rho u_0^2/2}$
∞	0	1.000 0	0
250	0.000 004 11	1.008 1	0.015 56
100	0.000 028 0	1.020 4	0.034 57
60	0.000 076 8	1.034 5	0.059 15
50	0.000 113 4	1.041 7	0.070 74
40	0.000 181 4	1.052 6	0.088 74
30	0.000 345 6	1.071 4	0.121 0
25	0.000 519 1	1.086 9	0.150 9
20	0.000 862 1	1.111 0	0.192 1
15	0.001 669	1.152 5	0.267 1
10	0.003 999	1.233 1	0.427 2
8	0.006 001	1.284 4	0.534 9
5	0.011 08	1.383 3	0.775 8
4	0.013 32	1.418 6	0.873 8
3	0.015 62	1.451 4	0.971 7
2	0.017 70	1.478 5	1.058 5
0	0.019 71	1.502 8	1.142 0

Table 3. $m=5$

t_1	σ	λ	$\frac{p_0-p}{\rho u_0^2/2}$
∞	0	1.000 0	0
75	0.000 002 84	1.006 7	0.011 48
25	0.000 026 72	1.020 4	0.033 96
10	0.000 184 4	1.052 6	0.090 11
5	0.000 867 9	1.110 9	0.192 8
4	0.001 443	1.141 9	0.248 4
3	0.002 744	1.193 8	0.352 3
2	0.006 004	1.284 7	0.538 0
1.5	0.009 116	1.349 6	0.690 0
1	0.013 43	1.422 5	0.888 3
0.6	0.017 14	1.475 2	1.051 8
0.4	0.018 64	1.494 9	1.119 5
0	0.020 01	1.512 0	1.180 0

where

$$C_1 = \frac{16(m-1)^2 \log m}{(m^2+1)\log m-(m^2-1)} \tag{47}$$

The value of C_2 can be determined from the pressure drop which corresponds to $\sigma=\sigma_L$. Table 4 gives the values of C_1 and C_2.

Table 4.

m	1.2	2	5
C_1	23.986 7	23.812 5	23.088 1
C_2	0.661 6	0.672 2	0.718 0
σ_L	0.019 62	0.019 71	0.020 01

Roy[8] has presented his calculation result that the value of C_2 for $m=3.33$, 2 and 1.43 are respectively 0.74, 0.72 and 0.71. These values are larger than that of the present analysis.

6. Experimental Apparatus

A sketch of experimental apparatus for measurement of the pressure drop is shown in Fig. 4. Water and air was used as working fluid for the present test runs. This apparatus was common to each fluid.

Water System:

Water is supplied from a feed pump to the overflow tank where constant water level is kept, and then enters in the lower tank. Annular pipes for test runs are connected with this tank and water runs upwards through annular space to the upper tank. Water level in the upper tank with level gauge is so adjusted by valves ① and ② that constant level is kept. The flow rate of water from the upper tank is measured by the weight method. Annular pipes including test section consist of two drawn brass tubes. The entrance of these tubes was so rounded that the uniform velocity profile at the entrance ($x=0$) could be obtained. The assembly of the entrance is shown in Fig. 5. The inner diameter of outer tube is 34.82 ± 0.03 millimeters, and the outer diameters of two inner tubes which are interchangeable are 31.75 ± 0.03 millimeters and 27.42 ± 0.04 millimeters, therefore the radius ratios were $m=1.0967\pm0.0020$ and 1.2699 ± 0.0030,

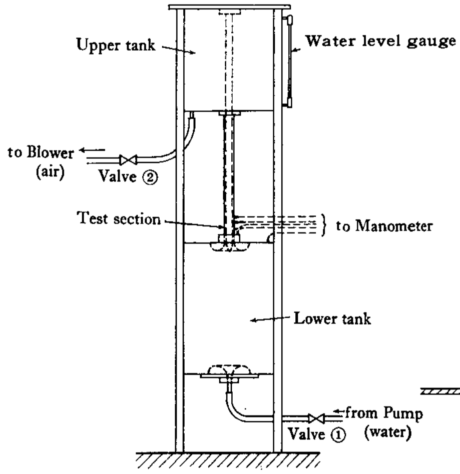

Fig. 4. Experimental apparatus

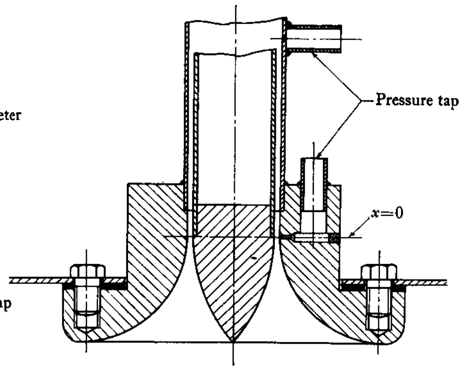

Fig. 5. Assembly of entrance

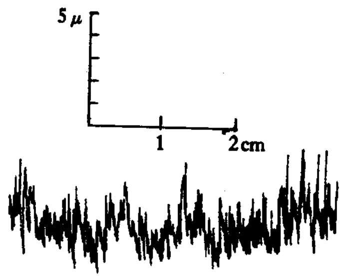

Fig. 6. Inspected result of tube surface

respectively. Fig. 6 shows a result obtained from the inspection of the outer surface of inner tube by the use of Kosaka's surface tester with tracer. It was proved that the roughness of surface in axial direction was so smooth that maximum roughness was about 5 microns. The pressure drop was measured by water manometer which was connected to seven pressure taps including the entrance ($x=0$). The pressure taps were located at $x=0$, 14.6, 29.6, 49.6, 70.0, 90.3 and 110.8 millimeters from the entrance. Since the pressure difference was very small, the measurement was made by means of cathetometer. The range of Reynolds number was limited to be lower than 1000 in order to maintain the condition of laminar flow.

Air System:

For test runs of air, the upper tank was connected with suction side of a centrifugal blower through a flow meter. This flow meter was calibrated by the volume method. The pressure drop was measured by the use of Betz-type manometer which was connected with the foregoing pressure taps. In this case, Reynolds number was also usually lower than 1000.

7. Experimental Results

Fig. 7 and 8 show the experimental results which were obtained on test runs for water and air, respectively. Each result shows that the measured values have a good agreement with the present analysis near the entrance, but are lower than the analytical values by about 10% for downstream. Murakawa's solution is appended to these figures for comparison, and his result

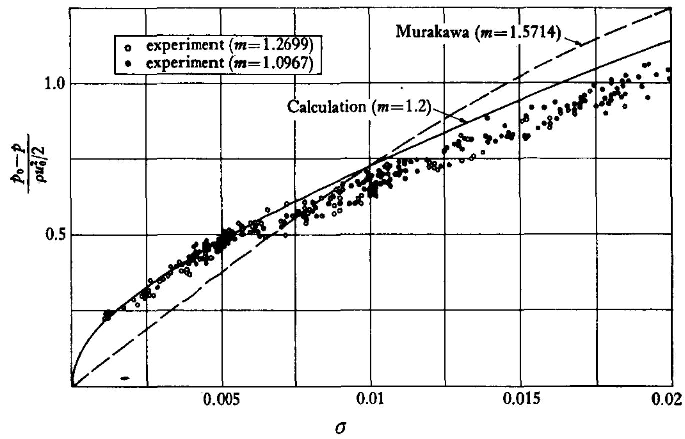

Fig. 7. Experimental results of pressure drop (water)

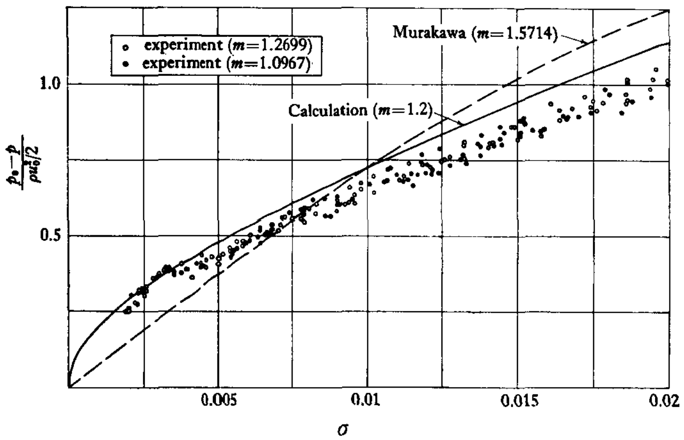

Fig. 8. Experimental results of pressure drop (air)

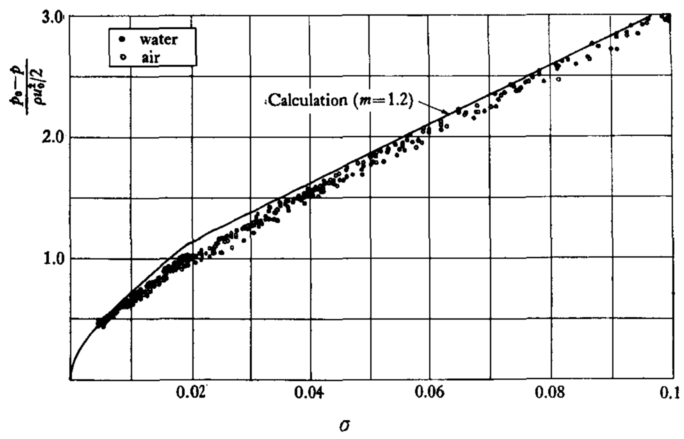

Fig. 9. Experimental results of pressure drop ($m=1.0967$)

appears to be too small near the entrance and to be large near the end of the inlet length. It may be considered that the experimental results of pressure drop are also unaffected by the radius ratio, though clear judgment can not be made because the radius ratios of test runs ($m=1.0967$ and 1.2699) have not a large difference and there are some discrepancy.

Fig. 9 shows an example of data of pressure drop for $\sigma>\sigma_L$. There exists a little difference of radius ratio between $m=1.2$ for the calculated value and $m=1.0967$ for the measured value, but a good agreement is observed, except the region where the calculated value has a discontinuous point, i.e. near the end of the inlet length. However, the measured value of C_2 in Eq. (46) is a little lower than that of analytical value, and considered to be about 0.62. And as shown in this figure, it may be presumed that the inlet length σ_L is 0.05～0.06 experimentally, while about 0.02 analytically.

8. Conclusion

The velocity distribution for the steady flow in the laminar inlet of a pipe with annular space are given by Eq. (12), and the distance from the pipe entrance, which corresponds to the given velocity distribution, can be estimated from Eq. (36). The pressure drop can be obtained from Eq. (39) in the inlet, and from Eq. (46) for $\sigma>\sigma_L$. As shown in the calculated examples, the inlet length and the pressure drop are almost unaffected by the radius ratio m. Therefore, σ_L may be evaluated practically to be 0.02.

Near the entrance, experimental results of pressure drop have a good agreement with calculated values. For downstream, experimental values are a little lower than analytical values, and near $\sigma=0.02$ this deviation is about 10% which is largest. Experimentally, C_2 in Eq. (46) may be evaluated to be 0.62, which is lower than calculated value by about 6%. And the inlet length σ_L may be observed experimentally to be 0.05～0.06, which is very longer than the calculated value.

Acknowledgement

The author is greatly indebted to Dr. M. Sibahayasi for his consistent guidance in this investigation and thanks Mr. M. Tsunano and the late Mr. T. Matsuo for their earnest assistances in the computations, and Mr. S. Tanimura and Mr. Y. Kawata in the experiments also.

This investigation has been subsidized by the Ministry of Education for the scientific research.

References

1) W.M. Kays: "*Numerical Solutions for Laminar-Flow Heat Transfer in Circular Tubes*", *Trans. of the ASME.*, vol. 77, 1955, p. 1265.

2) M. Sibahayasi and E. Sugino: "*On the Temperature Distribution at the Laminar Inlet in a Circular Pipe*", *Proc. of the 6th Japan National Congress for Appl. Mech.*, 1956, III-5, p. 389.
M. Sibahayasi and E. Sugino: "*Heat Transfer at the Laminar Inlet in a Circular Pipe*", *Proc. of the 7th Japan National Congress for Appl. Mech.*, 1957, III-1, p. 293.
M. Sibahayasi and E. Sugino: "*Nusselt Number for the Laminar Inlet in a Circular Pipe*", *Proc. of the 8th Japan National Congress for Appl. Mech.*, 1958, III-1, p. 339.

3) R.D. Cess and E.C. Shaffer: "*Laminar Heat Transfer Between Parallel Plates with an Unsymmetrically Prescribed Heat Flux at the Walls*", *Appl. Sci. Res.*, sec. A, vol. 9, 1960, p. 64.

4) L.S. Han: "*Simultaneous Developments of Temperature and Velocity Profiles in Flat Ducts*", *paper no.* 70, *International Heat Transfer Conference*, Boulder, Colorado, 1961.

5) R. Siegel and E.M. Sparrow: "*Simultaneous Development of Velocity and Temperature Distributions in a Flat Duct with Uniform Wall Heating*", *AIChE. Jour.*, vol. 5, no. 1, 1959, p. 73.

6) K. Murakawa: "*Theoretical Solutions of Heat Transfer in the Hydrodynamic Entrance Length of Double Pipes*", *Bull. of JSME.*, vol. 3, no. 11, 1960, p. 340.

7) K. Murakawa: "*Velocity Distribution over the Entry Length in Pipes with Annular Space*", *Trans. of the JSME.*, vol. 22, no. 117, 1956, p. 349.

8) D.N. Roy: "*Laminar Flow Near the Entry of Coaxial Tubes*", *Appl. Sci. Res.*, sec. A, vol. 14, 1965, p. 421.
9) H.L. Langhaar: "*Steady Flow in the Transition Length of a Straight Tube*", *Jour. Appl. Mech.*, vol. 9, no. 2, 1942, p. A-55.
10) L.S. Han: "*Hydrodynamic Entrance Lengths for Incompressible Laminar Flow in Rectangular Ducts*", *Jour. Appl. Mech.*, vol. 27, no. 3, 1960, p. 403.
11) K. Tomita: "*On the Flow through Pipes with Core and the Resistance to Flow*", *Trans. of the JSME.*, vol. 1, no. 5, 1935, p. 329.
12) S. Goldstein: "*Modern Developments in Fluid Dynamics*", Vol. 1, Oxford, 1938, p. 305.